CARBON 47 (2009) 2855–2864

available at www.sciencedirect.com

ScienceDirect

journal homepage: www.elsevier.com/locate/carbon

Understanding mercury binding on activated carbon

*Bihter Padak, Jennifer Wilcox**

Department of Energy Resources Engineering, Stanford University, 367 Panama St., Stanford, CA 94305-2220, United States

ARTICLE INFO

Article history:
Received 18 March 2009
Accepted 10 June 2009
Available online 18 June 2009

ABSTRACT

Understanding the mechanism by which mercury adsorbs on activated carbon is crucial to the design and fabrication of effective capture technologies. In this study, the possible binding mechanism of mercury (Hg) and its species, i.e., HgCl and $HgCl_2$ on activated carbon is investigated using *ab initio*-based energetic calculations. The activated carbon surface is modeled by a single graphene layer in which the edge atoms on the upper side are unsaturated in order to simulate the active sites. In some cases, chlorine atoms are placed at the edge sites to examine the effect of chlorine on the binding of Hg, HgCl and $HgCl_2$. It has been concluded that both HgCl and $HgCl_2$ can be adsorbed dissociatively or non-dissociatively. In the case of dissociative adsorption, it is energetically favorable for atomic Hg to desorb and energetically favorable for it to remain on the surface in the Hg^{1+} state, HgCl. The Hg^{2+} oxidized compound, $HgCl_2$ was not found to be stable on the surface. The most probable mercury species on the surface was found to be HgCl.

1. Introduction

Coal-fired power plants in the United States, with the capacity of just over 300 GW, are the greatest anthropogenic source of mercury emissions [1]. Mercury is a toxic metal that accumulates in the food chain and is considered a hazardous air pollutant (HAP) by The Clean Air Act (CAA) of 1990.[1] Mercury has severe health effects and may cause central nervous system damage, pulmonary and renal failure, severe respiratory damage, blindness and chromosome damage [2,3]. The United States Environmental Protection Agency (USEPA) promulgated the Clean Air Mercury Rule (CAMR) in 2005 to permanently reduce the mercury emissions from coal-fired power plants [4]. Although this rule was vacated by the Courts in February 2008,[2] currently 14 states still have mercury emissions controls in place for coal-fired power plants [5].

Various methods are applied for capturing different forms of mercury, i.e., elemental (Hg), oxidized and particulate-bound. Particulate-bound can be removed through electrostatic precipitators and fabric filters while oxidized mercury can be captured by flue gas desulfurization scrubbing units. Activated carbon, when injected into the gas stream of coal-fired boilers, is effective in capturing mercury through adsorption processes [1]. A detailed literature survey of Hg removal by activated carbon injection is given elsewhere [6].

Experimental studies have been previously carried out to understand the mechanism of mercury binding on activated carbon surfaces [7–10] and it has been made clear that the reaction mechanisms involved in mercury capture are very complex [7,10]. Hutson et al. [10] reported the factors that play a role in determining the rate and mechanism of mercury binding, to be gas-phase speciation of mercury, presence of other potentially competing flue gas components, flue gas temperature, and the presence and type of active binding sites on the sorbent. They have used X-ray Absorption Spectroscopy (XAS) and X-ray Photoelectron Spectroscopy (XPS) to characterize mercury binding on various types of activated carbon. Mercury was found to be bound on carbon at the

* *Corresponding author:* Fax: +1 650 725 2099.
E-mail address: wilcoxj@stanford.edu (J. Wilcox).

[1] [Cited 2009 March 7]; Available from <http://www.epa.gov/air/caa/>.

[2] [Cited 2009 March 7]; Available from <http://www.epa.gov/camr/>.

0008-6223/$ - see front matter © 2009 Elsevier Ltd. All rights reserved.
doi:10.1016/j.carbon.2009.06.029

chlorinated or brominated sites. No elemental mercury was observed on the activated carbon surface. Considering the fact that there is no homogeneous mercury oxidation occurring in their system, there must be heterogeneous oxidation with subsequent binding on the surface. In another X-ray Absorption Fine Structure (XAFS) study, Huggins and coworkers [8] also observed that there is little or no elemental mercury present in the sorbent materials and concluded that physisorption is not involved in adsorption of mercury at the low temperature conditions of their experiments. From these results, they infer that an oxidation process, either in the gas-phase or simultaneously as the mercury atom interacts with the sorbent, is involved in the capture of elemental mercury. In the case of chemically treated sorbents, mercury sorption is predicted to occur entirely by chemisorption. Furthermore, XANES (X-ray Absorption Near-Edge Structure) spectra indicates the formation of Hg–I, Hg–Cl, Hg–S and Hg–O. According to Laumb et al. [9], Cl and S are two of the most important elements when dealing with mercury capture on activated carbon.

Huggins et al. [7] have studied the sorption of Hg and $HgCl_2$ by three activated carbons using XAFS spectroscopy and found that a different mechanism is responsible for the mercury sorption by each different type of activated carbon. Activated carbons used in their experiments were a lignite-derived activated carbon (LAC), an iodine-activated carbon (IAC), and a sulfur-activated carbon (SAC). When the carbons were exposed to the flue gas containing elemental mercury, Hg–S or Hg–Cl bonding was observed in SAC and LAC carbons and Hg–I bonding in the IAC carbon. Exposing LAC to the flue gas containing $HgCl_2$ revealed that mercury chloride is the most likely sorbed mercury species. In the case of IAC, Hg–I was observed on the carbon. According to the authors, $HgCl_2$ must have decomposed to an Hg species in the gas-phase or reacted at the active site, releasing Cl, to form the Hg–I complex. These results indicate that the speciation of the sorbed mercury is controlled by the site-activating agent on the carbon surface.

Although many experimental studies have been performed to investigate mercury adsorption on activated carbon, there are a limited number of theoretical studies on this subject. Steckel [11] has investigated the interactions between elemental mercury and a single benzene ring, which is quite limited in its potential for representing an accurate carbon surface. However, this study is the first to begin the investigations required for elucidating the mechanism by which elemental mercury binds to carbon. In a previous study [6], authors have conducted an *ab initio*-based investigation involving the adsorption of elemental mercury on halogen-embedded activated carbon. The effects of activated carbon's different surface functional groups and halogens on elemental mercury adsorption have been examined and the addition of halogen atoms has been found to increase activated carbon's mercury adsorption capacity.

Nonetheless, the mechanism by which mercury adsorbs on activated carbon is not exactly known and its understanding is crucial to the design and fabrication of effective capture technologies for mercury. The objective of the current study is to apply theoretical-based cluster modeling to examine the possible binding mechanism of mercury on activated carbon.

2. Computational methodology

Binding mechanisms of Hg, HgCl and $HgCl_2$ on simulated activated carbon surfaces and the effects of adsorbed Cl were investigated by following a thermodynamic approach. Energies of different possible surface complexes and possible products are compared and dominant pathways are determined relatively.

The Gaussian03 software package [12] was used for all of the energy calculations in this work. Density Functional Theory (DFT) was employed due to its balanced computational efficiency and accuracy. B3LYP is known to produce fairly accurate bond energies and thermodynamic properties of reactions [13,14]. Also, it has small spin contamination compared to other methods such as Hartree–Fock (HF) [15]. Montoya et al. [15] have illustrated that spin contamination in the unrestricted B3LYP is reasonably small and has acceptable minor effects on the energetic properties of graphene layers. They have also shown that the differences in both adsorption geometry and binding energy between the unrestricted and restricted open-shell wave function are small. The B3LYP method has been employed in many studies [13–20], in which a carbonaceous surface is simulated, along with the 6-31G(d) basis set and has been shown to provide accurate energetic properties of carbon–oxygen complexes [13,14,16]. According to Radovic and Bockrath [19], this level of theory is a reasonable compromise that minimizes spin contamination, includes configurational interaction, and accomplishes the calculations at acceptable computational expense.

In this study, considering that mercury has eighty electrons, to account for relativistic effects a basis set with the inner electrons substituted by an effective-core potential (ECP) was chosen. Beck's three-parameter functional with a Lee–Yang–Parr gradient-corrected correlation functional (B3LYP) with LANL2DZ basis set which uses an all-electron description for the first-row elements and an ECP for inner electrons and double-ζ quality valence functions for the heavier elements was used for the energy predictions [21–23].

Each structure is optimized through the investigation of stable energies at different multiplicities and the ground state is determined by the lowest energy complex among the different electronic states.

3. Results and discussion

3.1. *Modeling the activated carbon surface*

The activated carbon surface is modeled by a single graphene layer in which the edge atoms on the upper side are unsaturated in order to simulate the active sites. This model has been used in several studies of different applications to simulate carbonaceous surfaces [13–18,24]. Chen and Yang [25] have compared six graphite models with increasing sizes using the HF method and found the model $C_{25}H_9$ to be the most suitable model to simulate the graphite structure, yielding structural parameters close to the experimental data. On the other hand, Montoya et al. [13] decreased the molecular system and used $C_{18}H_8$ as their model, employing the B3LYP method. The conclusion was that even at this size, the struc-

tural parameters for the carbon–nitrogen models were in agreement with the experimental data. Both Chen et al. [25] and Montoya et al. [14] have shown that the reactivity of the carbon model does not depend strongly on the molecular size. The reactivity of the active sites, which are the unsaturated carbon atoms at the edge of the graphene layers, depends mainly on its local shape rather than on the size of the graphene cluster [14].

Also, analysis of a single graphene layer is a convenient and reasonable starting point when studying the reactivity of carbon surfaces [18]. In an early *ab initio* study, comparison of two and three dimensional models for the graphite lattice predicted a weak interaction between atoms in adjacent stacking planes, leading to the conclusion that treating graphite as a two dimensional solid is a reasonable approximation [26]. Yang and Yang [20] have conducted an *ab initio* molecular orbital study on the adsorption of atomic hydrogen on graphite and concluded that the strength of chemisorption is higher on the edge planes than the basal planes, following the order: zigzag edge > armchair edge > basal-plane. Another study on the adsorption of oxygen on boron-substituted graphite has yielded that zigzag sites are more reactive than armchair sites, due to the existence of unpaired electrons on zigzag edges, while no such electrons are found on armchair edges [27]. Armchair sites are of the carbyne type, while zigzag sites are of the carbene type and they posses two nonbonding electrons [19]. Radovic and Bockrath [19] have studied the chemical nature of the graphene edges and stated that "complete saturation with H or other heteroatoms is unrealistic and not all graphene edge sites are saturated with H." There has also been experimental evidence on the existence of partially-stabilized radical sites at graphene edges [28]. Although O_2 chemisorption is known to occur readily at room temperature, it has been shown that oxygen-free carbon edge sites can still exist after exposure to air [19,28]. In addition to these, the existence of the carbene sites has been supported by another study, where it was proposed that zigzag Lewis basic carbene reacts with oxidized Hg species [29].

Based on the previous studies, it is a reasonable approximation to use a graphene model where the zigzag edges are unsaturated to simulate the active sites. The optimized geometry of the graphene model (G) is shown in Fig. 1 with the optimized parameters given in Table 1. Bond distances and angles of the optimized structure are in good agreement with the experimental values of graphite [30].

Another model includes a chlorine atom placed at the edge site to determine the effect of chlorine on the binding of mercury and its species. XPS studies conducted to examine

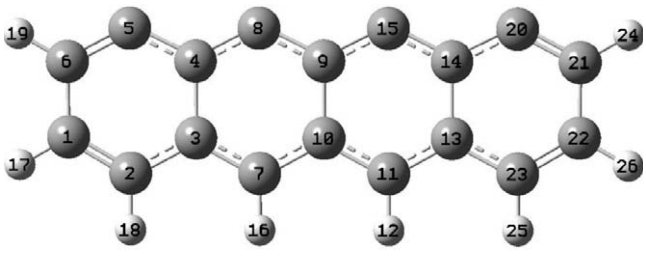

Fig. 1 – Optimized geometry of graphene (G).

Table 1 – Optimized parameters of graphene model (bond lengths in Å and angles in degrees) av: average.

Parameter (av)	Model	Exp [29]
C–C	1.42	1.42
C–H	1.09	1.07
∠C–C–C	120	120
∠C–C–H	119.7	120.0

chlorinated-activated carbons showed that chlorine was localized at the edges of graphene layers [31]. Based on this, the optimization of the chlorine atom at different sites of the graphene model yielded the structures G–Cl(1) and G–Cl(2) as shown in Fig. 2. Other models shown in Fig. 2, which consist of two Cl atoms on the surface, were also employed.

The binding of Hg, HgCl and $HgCl_2$ at different sites of graphene and graphene–Cl models described above is studied and a possible binding mechanism is suggested. Binding energies of mercury species on simulated activated carbon were calculated using Eq. (1),

$$\text{Binding energy} = E(\text{AC–Hg}) - [E(\text{Hg}) + E(\text{AC})] \quad (1)$$

In addition, bond populations are calculated by performing a Mulliken population analysis. Mulliken population is used for charge determination and as a measure of bond strength. Although absolute values of populations have little physical meaning, their relative values can be useful. For example, positive and negative values of bond population mean that the atoms are bonded or antibonded, respectively. A large positive value indicates that the bond is largely covalent, whereas there is no interaction between the two atoms if the bond population is close to zero [27].

Bond populations for the graphene (G) and graphene–Cl models are given in Table 2. The populations for only the bonds of interest are reported here.

When Cl is adsorbed on the surface, the C(8)–C(9) bond is elongated. The bond length increases from 1.401 to 1.415 and the bond population decreases from 0.302 to 0.038. The decrease in the bond population shows that a portion of the bonding electrons were transferred to the adsorbed Cl atom, thus weakening the bond. Similarly, the C(4)–C(8) bond is also weakened. The bond length increases from 1.388 to 1.401 and the bond population decrease from 0.393 to 0.175.

3.2. *Binding of Hg on graphene*

The interaction of Hg with different sites of graphene was examined. Different locations of Hg on the graphene model (G) are shown as "a", "b" and "c" in Fig. 3. Both "b" and "c" yielded the same surface complex shown as BC whereas "a" yielded the complex A. The binding energies of Hg with A and BC are found to be 14.28 kcal/mol and 14.84 kcal/mol, respectively, indicating that the stabilities of these structures are very similar.

The bond populations of Hg on the graphene model are given in Table 2. For the structure BC, the C(8)–C(9) and C(9)–C(15) bonds are weakened by the adsorption of Hg, with their bonding populations decreasing from 0.30 to 0.11. Comparing the bond populations of the Hg atom with the near C atoms, it

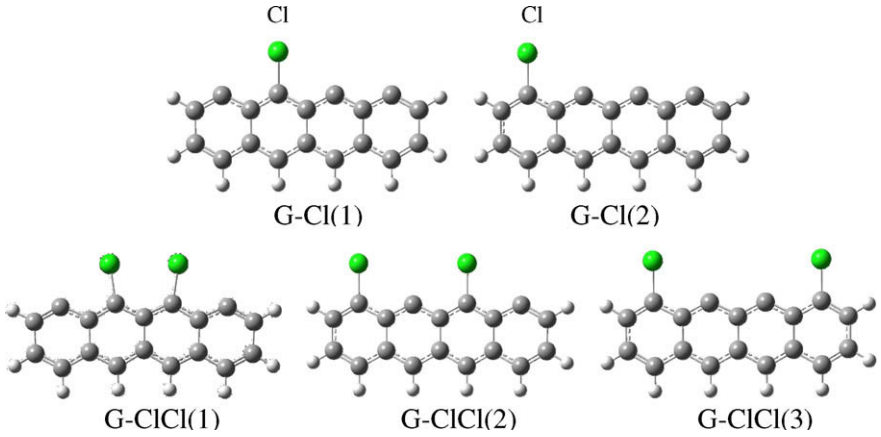

Fig. 2 – Graphene models with chlorine.

Table 2 – Bonding Mulliken population analysis for graphene, graphene–Cl and Hg on graphene (only bonds of interest are reported).

	Graphene	Graphene–Cl	Hg on graphene	
	G	G–Cl (1)	BC	A
C(6)–C(5)	0.486	0.516	0.489	0.497
C(5)–C(4)	0.342	0.332	0.336	0.332
C(4)–C(8)	0.393	0.175	0.458	0.408
C(8)–C(9)	0.302	0.038	0.107	0.308
C(9)–C(15)	0.302	0.313	0.108	0.374
C(15)–C(14)	0.393	0.450	0.458	0.187
C(14)–C(20)	0.342	0.339	0.338	0.208
C(20)–C(21)	0.486	0.490	0.490	0.484
Cl–C(8)		0.416		
Hg–C(8)			0.251	
Hg–C(9)			−0.184	
Hg–C(15)			0.251	0.252
Hg–C(14)				−0.183
Hg–C(20)				0.258

becomes clear that Hg is interacting with the two carbon atoms C(8) and C(15), and there is no significant interaction with C(9). Similarly, for the structure A, Hg is interacting with the two carbon atoms C(15) and C(20).

3.2.1. *Binding of Hg on graphene–Cl*

The G–Cl model is also employed to illustrate the effects of adsorbed chlorine on the surface. Different locations of Hg are shown in Fig. 4 with the possible surface intermediates D, E, F and GH. Bonding populations of these structures are given in Table 3. Both g and h converged to the same minimum energy yielding the intermediate GH. In this case, the binding energy of Hg is 14.36 kcal/mol, which is similar to the value of Hg on graphene. The intermediate F is possibly a result of a surface reaction between Hg and Cl yielding HgCl on the surface.

From these four surface intermediates possible final structures can be suggested as a result of desorption. One possibility is that Hg can be desorbed and Cl remains on the surface or vice versa. Another possibility is that HgCl desorbs from

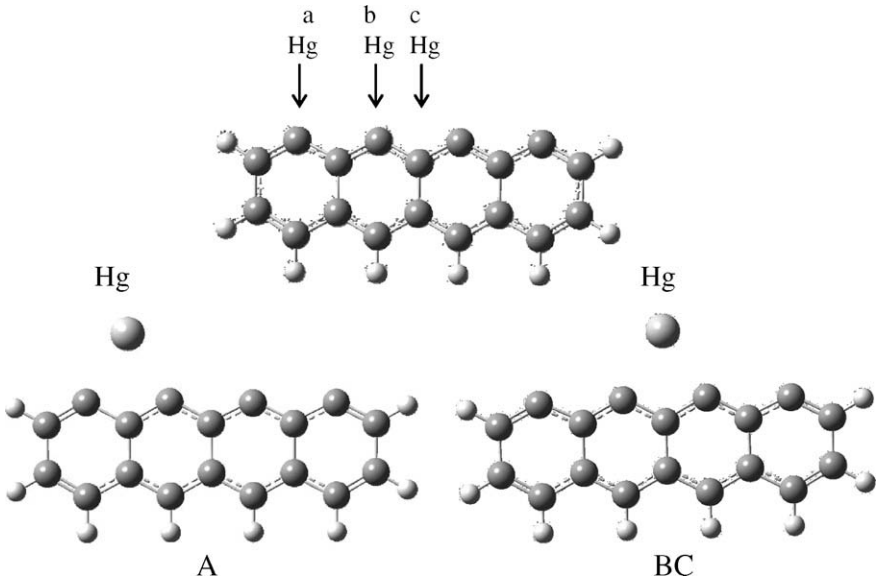

Fig. 3 – Binding of Hg at different sites of graphene (G).

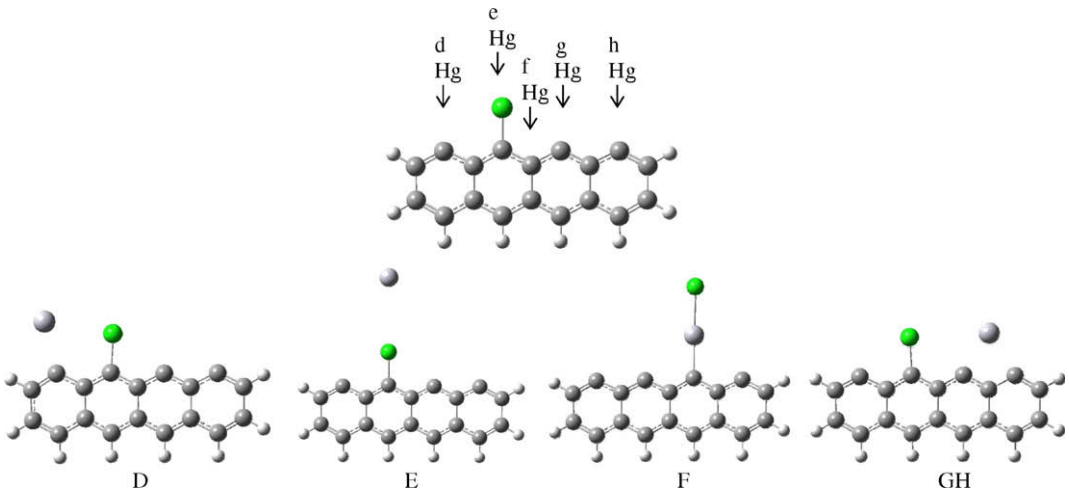

Fig. 4 – Binding of Hg at different sites of G–Cl model.

intermediate F. The possible pathways including reactants, intermediates and products are shown in the energy diagram given in Fig. 5. All energy values are given relative to the reactants.

From examining the energy diagram, it seems that the stability of the intermediates are in the order of GH > D > F > E. The most likely structure is complex GH, since its path is more exothermic than that of the others. It appears from the energy diagram that complex E is not as likely to form. Although the formation of F is not as exothermic as D and GH, there is likelihood that F can be formed as well. It is clear from Fig. 5 that desorption from these surface complexes is endothermic and not likely to occur without adding energy to the system. The desorption pathways of Cl and HgCl from the GH complex are highly endothermic, but there is a possibility that it may go back to the reactants with the desorption of Hg. Pathways of Cl desorption from D are shown in the energy diagram; however, it is more probable that these intermediates will go back to the reactants or remain as stabilized intermediates. Careful examination of complex F indicates that once HgCl is on the surface it does not desorb easily. This can also be concluded from the population analysis. The bond population of Hg–C in F is higher compared to the Hg–C population in the other structures, indicating that HgCl is strongly bound to the surface. Although the binding energy for the structure F is lower compared to GH, the interaction between Hg and C is stronger in F. A similar phenomena has been observed by Nilsson and Pettersson [32], where they have concluded that "a small adsorption energy cannot by itself be used to conclude a weak interaction". They have shown that there can still be surprisingly large and important chemical bonding interactions with the surface that are beyond a physical adsorption picture.

3.3. *Binding of HgCl on graphene*

In the same manner, the interaction of HgCl with different sites of graphene was examined allowing HgCl to approach

Table 3 – Bonding Mulliken population analysis for Hg on graphene–Cl and HgCl on graphene (only bonds of interest are reported).

	Hg on graphene–Cl				HgCl on graphene							
	D	E	F	GH	1A	1B	1C	1D	2AB	2C	2D	3C
C(6)–C(5)	0.392	0.517	0.498	0.525	0.392	0.432	0.388	0.418	0.490	0.503	0.515	0.437
C(5)–C(4)	0.297	0.331	0.334	0.325	0.298	0.062	0.197	0.081	0.217	0.300	0.332	0.380
C(4)–C(8)	0.128	0.175	0.430	0.227	0.128	0.337	0.363	0.413	0.247	0.263	0.172	0.338
C(8)–C(9)	0.111	0.034	0.250	0.023	0.111	0.253	0.350	0.374	0.377	0.161	0.034	0.209
C(9)–C(15)	0.289	0.311	0.164	0.376	0.289	0.284	0.298	0.298	0.023	0.249	0.310	0.209
C(15)–C(14)	0.470	0.451	0.261	0.247	0.470	0.418	0.417	0.407	0.227	0.430	0.449	0.338
C(14)–C(20)	0.334	0.339	0.300	0.217	0.334	0.327	0.341	0.340	0.325	0.335	0.340	0.380
C(20)–C(21)	0.496	0.492	0.503	0.489	0.496	0.498	0.494	0.494	0.525	0.498	0.490	0.437
Cl–C*	0.367	0.403		0.388	0.367	0.309		0.333	0.388		0.406	
Hg–Cl	0.005	0.006	0.265	0.008	0.006	0.005	0.259	0.007	0.008	0.265	0.006	0.252
Hg–C(5)	0.154				0.153		0.389		0.255			
Hg–C(15)			0.368	0.255								0.223
Hg–C(8)						0.163			0.255	0.369		0.223
Hg–C(20)				0.255								

* Nearest carbon.

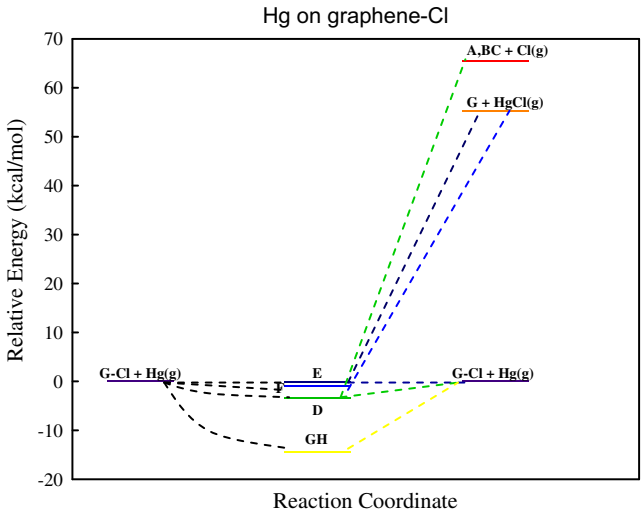

Fig. 5 – Energy diagram for different pathways of Hg on G–Cl.

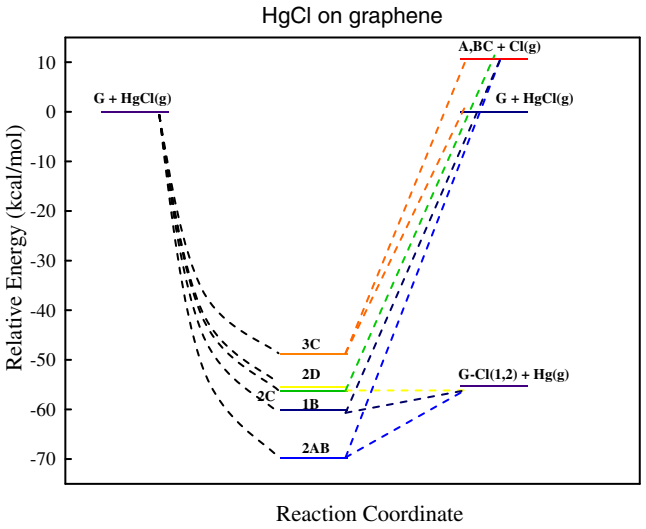

Fig. 7 – Energy diagram for different pathways of HgCl on G.

graphene from different directions. Unique locations and orientations of HgCl on the graphene model (G) are shown in Fig. 6 with the possible surface intermediates 1A, 1B, 1C, 1D, 2AB, 2C, 2D and 3C. Depending on the orientation of HgCl, it may or may not be adsorbed dissociatively.

These surface intermediates and possible final structures are shown in the energy diagram of Fig. 7, with the energies relative to the reactants. Bonding populations of these structures are given in Table 3.

Similar surface complexes are obtained to those with Hg on G–Cl, but with higher binding energies. For example, the complex GH with a binding energy of 14.36 kcal/mol is optimized with Hg on the G–Cl surface. The same complex is also obtained through the optimization of HgCl on the G surface

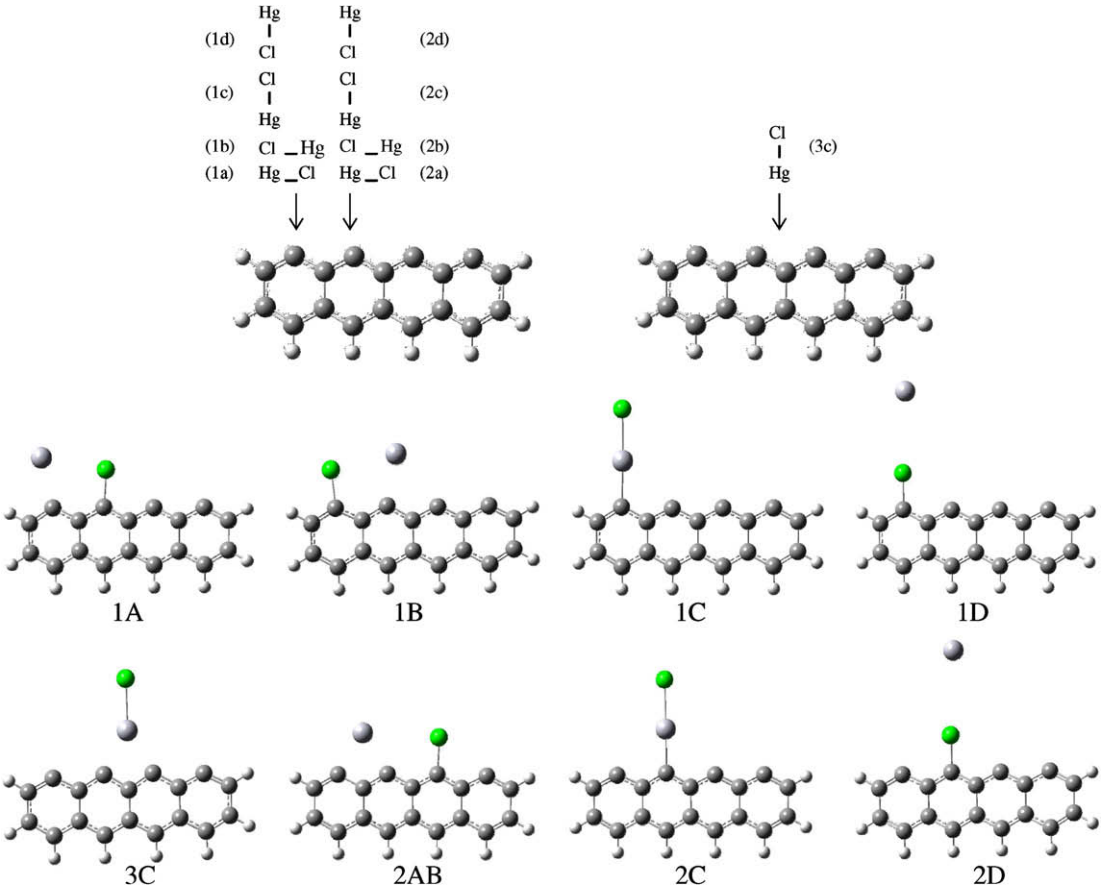

Fig. 6 – Binding of HgCl at different sites of G.

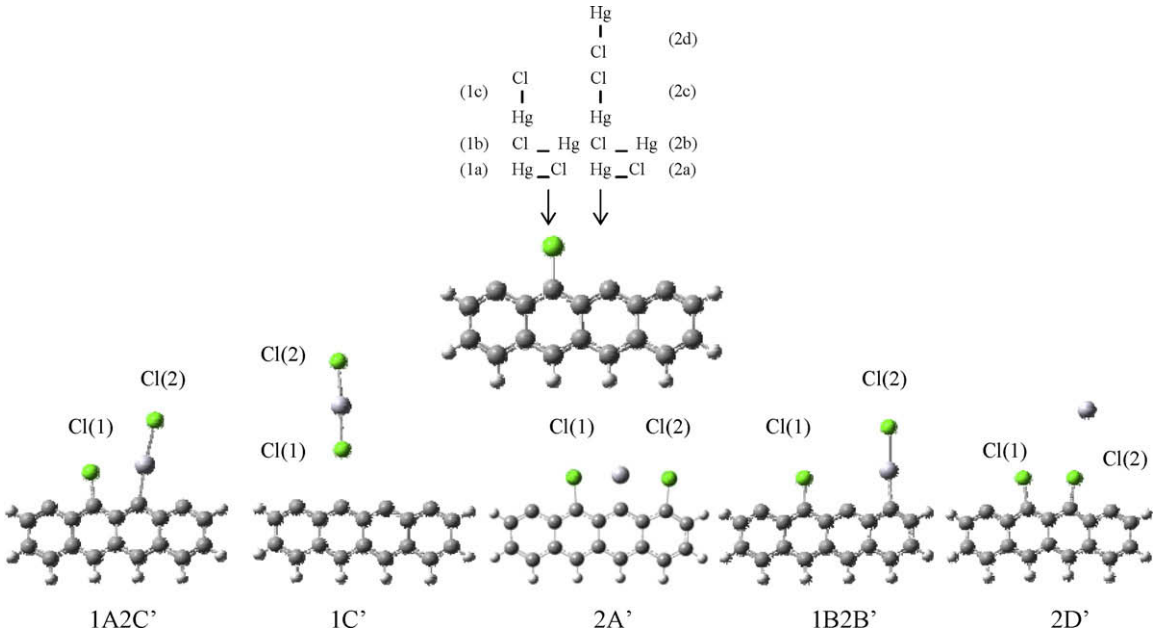

Fig. 8 – Binding of HgCl at different sites of G–Cl.

with two different orientations, i.e., 2a and 2b, yielding the complex 2AB with a binding energy of 69.70 kcal/mol.

The stability of the surface complexes are in the order of 2AB > 1B > 2C > 2D > 3C, which implies that HgCl is likely to adsorb dissociatively. However, it is clear from the energy diagram that Hg can desorb from the surface. On the other hand, the desorption of HgCl is highly endothermic which shows that once it is adsorbed it remains on the surface. As was explained in the previous section, the bonding population analysis indicates that HgCl is strongly bound to the surface.

3.3.1. *Binding of HgCl on graphene–Cl*

The interaction between HgCl and the graphene–Cl model was also investigated. Having HgCl approaching the G–Cl surface with different orientations, shown in Fig. 8, yielded the surface intermediates, 1A2C′, 1C′, 2A′, 1B2B′, 2D′.

Two different orientations of HgCl, i.e., 1a and 2c, yielded the same surface complex, 1A2C′, which is the most stable structure, with a binding energy of 55.00 kcal/mol. Similar to HgCl on the graphene model, when the G–Cl model is used HgCl may or may not adsorb dissociatively. A similar trend to the adsorption on graphene is observed, such that Hg can be desorbed in the case of dissociative adsorption, while HgCl remains on the surface. Although 2A′ has similar exothermicity to 1A2C′ and 1B2B′, it appears from the bond populations of Hg–C (provided in Table 4) that HgCl in 1A2C′ and 1B2B′ is more strongly bound on the surface than Hg in 2A′.

Table 4 – Bonding Mulliken population analysis for HgCl on graphene–Cl and $HgCl_2$ on graphene (only bonds of interest are reported).

	HgCl on graphene–Cl					$HgCl_2$ on graphene				
	1A2C′	1C′	2A′	1B2B′	2D′	1A″	1B″	2A″	2B″	3B4B″
C(6)–C(5)	0.531	0.481	0.525	0.520	0.526	0.425	0.365	0.428	0.480	0.524
C(5)–C(4)	0.328	0.348	0.330	0.325	0.333	0.076	0.089	0.086	0.348	0.356
C(4)–C(8)	0.250	0.402	0.219	0.195	0.186	0.365	0.344	0.445	0.399	0.446
C(8)–C(9)	−0.042	0.310	0.263	0.000	0.032	0.299	0.294	0.188	0.313	0.309
C(9)–C(15)	0.172	0.317	0.298	0.356	0.035	0.026	0.218	0.186	0.316	0.071
C(15)–C(14)	0.251	0.390	0.367	0.430	0.185	0.216	0.334	0.445	0.388	0.200
C(14)–C(20)	0.293	0.340	0.075	0.186	0.333	0.330	0.379	0.085	0.340	0.314
C(20)–C(21)	0.496	0.488	0.426	0.385	0.527	0.522	0.436	0.428	0.487	0.516
Cl(1)–C*	0.373	−0.002	0.379	0.420	0.430	0.314	0.348	0.324	0.0001	0.357
Cl(2)–C*			0.315		0.417	0.380		0.324		
Hg–Cl(2)	0.266	0.248	0.002	0.261	0.006	0.001	0.254	0.010	0.250	0.045
Hg–Cl(1)	0.018	0.237	0.001	0.004	0.001	0.002	0.007	0.010	0.240	−0.005
Hg–C(15)	0.371		0.148				0.218	0.252		
Hg–C(8)						0.149	0.213	0.252		
Hg–C(20)				0.390						

* Nearest carbon.

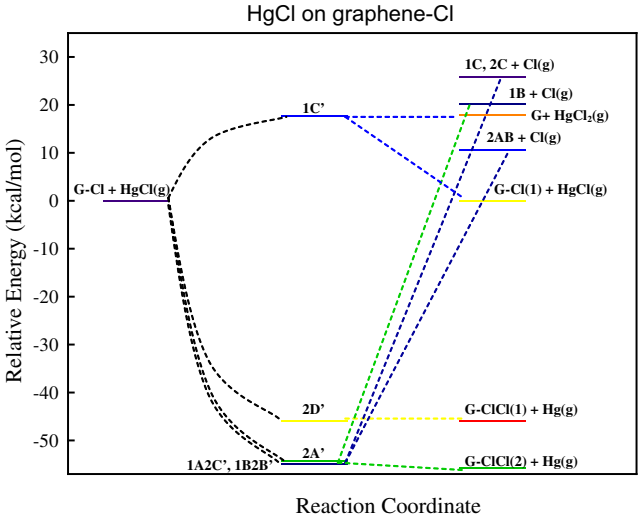

Fig. 9 – Energy diagram for different pathways of HgCl on G–Cl.

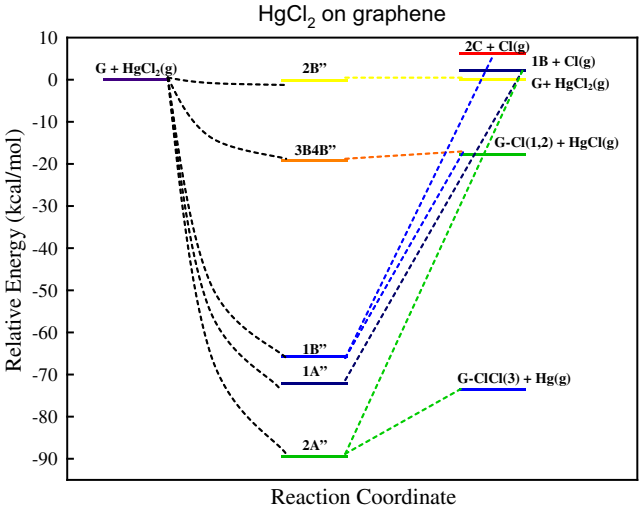

Fig. 11 – Energy diagram for different pathways of $HgCl_2$ on G.

Additionally, HgCl can react with a Cl atom on the surface to form $HgCl_2$. From the energy diagram pictured in Fig. 9, the latter pathway is not very likely, since it is endothermic. Even if $HgCl_2$ is formed on the surface it is not stable, and can easily desorb or return to the reactants. From the bond populations in Table 4, it appears that there is no interaction between the $HgCl_2$ molecules with the surface, because population of Cl–C is close the zero.

3.4. *Binding of $HgCl_2$ on graphene*

The optimization of $HgCl_2$ with different orientations on the grapheme model yielded the surface intermediates, 1A″, 1B″, 2A″, 2B″ and 3B4B″ as shown in Fig. 10. Similar surface complexes are obtained to those with HgCl on G–Cl, but with higher binding energies.

Close examination of the energy diagram provided in Fig. 11, indicates that complexes 2A″ and 1A″ are the most likely structures to form. However, it is possible that Hg can desorb. Especially in the case of 1A″, the interaction of Hg and C is weak and Hg has no significant interaction with Cl atoms, based on the bond populations given in Table 4. In addition to this, it is clear from the energy diagram that the desorption of Hg from 1A″ is exothermic and is likely to occur.

Another possibility is that $HgCl_2$ can form the surface intermediate 2B″ with a very small binding energy of 0.25 kcal/mol and almost zero bond population of Cl–C, implying that $HgCl_2$ is not stable on the surface and this surface intermediate can return to the reactants easily with the desorption of $HgCl_2$. Rather, it is likely that $HgCl_2$ dissociates and adsorbs as HgCl as in 1B″. Experiments conducted at EERC [7] have revealed that $HgCl_2$ decomposes at the active sites of carbon. XAFS experiments have showed that, under gas-phase $HgCl_2$, the most likely sorbed mercury species is HgCl, which agrees with the predictions of the current simulations.

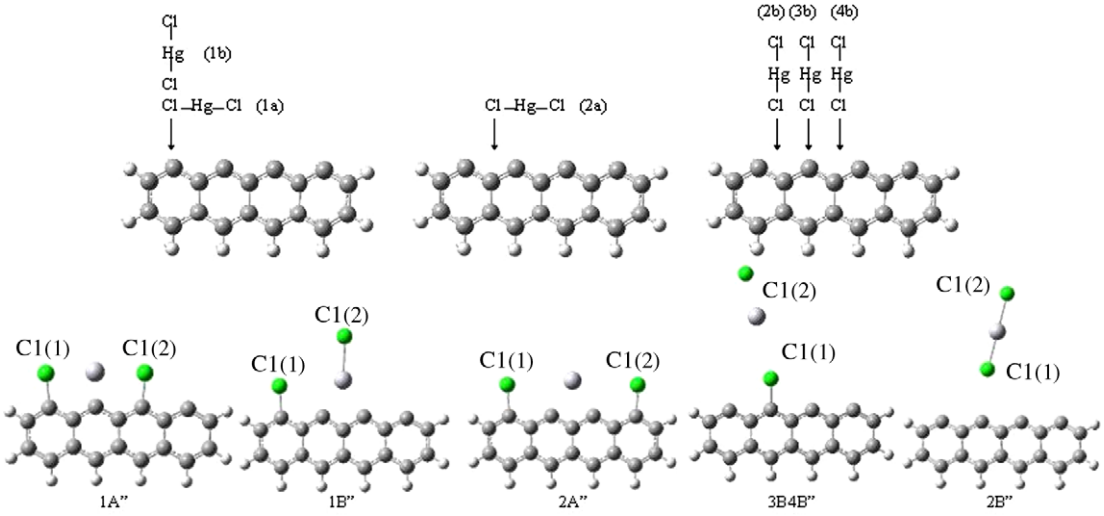

Fig. 10 – Binding of $HgCl_2$ at different sites of G.

4. Conclusions

A thermodynamic approach is followed to examine the binding mechanism of mercury and oxidized mercury species such as HgCl and $HgCl_2$ on a simulated carbon surface with and without Cl. Energies of different possible surface complexes and possible products are compared and dominant pathways are determined relatively. It is important to note that transition states along these pathways are not determined and the current investigation is solely of a thermodynamic nature.

In all of the cases, chlorine is bound strongly on the surface and it does not desorb. Both HgCl and $HgCl_2$ can be adsorbed dissociatively or non-dissociatively. In the case of dissociative adsorption, Hg can desorb while HgCl remains on the surface. The compound, $HgCl_2$ was not found to be stable on the surface. Even if it is formed on the surface, it can easily desorb or return to the reactant species. The most probable mercury species on the surface was found to be HgCl which has also been shown by experiments [7].

These observations serve to highlight the complexity of the binding mechanism of mercury species on activated carbon surfaces. Not only mercury–chlorine species are present in the flue gas but also mercury–bromine species exist and play a significant role in mercury capture by activated carbon. Further investigations will be carried out to examine the binding of HgBr and $HgBr_2$ on the simulated carbon surface and all dominant pathways will be combined to determine a complete binding mechanism of mercury species on simulated activated carbon surfaces. Understanding the mechanism by which mercury adsorbs on activated carbon would be useful to the design and fabrication of effective control technologies for mercury.

Acknowledgements

The computations were carried out on the Stanford CEES (Center for Computational Earth and Environmental Science) grid. This material is based upon work supported by the National Science Foundation under Grant No. 0448758.

REFERENCES

[1] Control of mercury emissions from coal fired electric utility boilers: an update. Air pollution prevention and control division. US Environmental Protection Agency; 2005.
[2] Berglund F, Bertin M. Chemical fallout. ILThomas: Springfield; 1969.
[3] WHO. Environmental health criteria 101, methylmercury. Geneva: World Health Organization; 1990. p. 68–102.
[4] US Environmental Protection Agency. Fact sheet: EPA's clean air mercury rule. Washington, DC; 2005.
[5] Slaughter C. Tutorial on mercury regulations: demystifying the law. In: Proceedings of the clearwater clean coal conference. Clearwater, FL; 2009.
[6] Padak B, Brunetti M, Lewis A, Wilcox J. Mercury binding on activated carbon. Environ Prog 2006;25:319–26.
[7] Huggins FE, Huffman GP, Dunham GE, Senior CL. XAFS examination of mercury sorption on three activated carbons. Energy Fuels 1999;13(1):114–21.
[8] Huggins FE, Yapa N, Huffman GP, Senior CL. XAFS characterization of mercury captured from combustion gases on sorbents at low temperatures. Fuel Process Technol 2003;82(2–3):167–96.
[9] Laumb JD, Benson SA, Olson EA. X-ray photoelectron spectroscopy analysis of mercury sorbent surface chemistry. Fuel Process Technol 2004;85(6–7):577–85.
[10] Hutson ND, Atwood BC, Scheckel KG. XAS and XPS characterization of mercury binding on brominated activated carbon. Environ Sci Technol 2007;41(5):1747–52.
[11] Steckel JA. Ab initio modelling of neutral and cationic Hg–benzene complexes. Chem Phys Lett 2005;409(4–6):322–30.
[12] Frisch MJ, Trucks GW, Schlegel HB, Scuseria GE, Robb MA, Cheeseman JR, et al. Gaussian 03, revision B.04. Pittsburgh, PA: Gaussian Inc.; 2003.
[13] Montoya A, Truong TN, Sarofim AF. Application of density functional theory to the study of the reaction of NO with char-bound nitrogen during combustion. J Phys Chem A 2000;104:8409–17.
[14] Montoya A, Truong TT, Mondragon F, Truong TN. CO desorption from oxygen species on carbonaceous surface: 1. Effects of the local structure of the active site and the surface coverage. J Phys Chem A 2001;105:6757–64.
[15] Montoya A, Truong TN, Sarofim AF. Spin contamination in Hartre–Fock and density functional theory wavefunctions in modeling of adsorption on graphite. J Phys Chem A 2000;104:6108–10.
[16] Montoya A, Mondragon F, Truong TN. First principles kinetics of CO desorption from oxygen species on carbonaceous surface. J Phys Chem A 2002;106:4236–9.
[17] Wu X, Radovic LR. Ab initio molecular orbital study on the electronic structures and reactivity of boron-substituted carbon. J Phys Chem A 2004;108:9180–7.
[18] Radovic LR. The mechanism of CO_2 chemisorption on zigzag carbon active sites: a computational chemistry study. Carbon 2005;43:907–15.
[19] Radovic LR, Bockrath B. On the chemical nature of graphene edges: origin of stability and potential for magnetism in carbon materials. J Am Chem Soc 2005;127:5917–27.
[20] Yang FH, Yang RT. Ab initio molecular orbital study of adsorption of atomic hydrogen on graphite: insight into hydrogen storage in carbon nanotubes. Carbon 2002;40:437–44.
[21] Hay PJ, Wadt WR. Ab initio effective core potentials for molecular calculations. Potentials for the transition metal atoms Sc to Hg. J Chem Phys 1985;82(1):270–83.
[22] Hay PJ, Wadt WR. Ab initio effective core potentials for molecular calculations. Potentials for K to Au including the outermost core orbitals. J Chem Phys 1985;82(1):299–310.
[23] Wadt WR, Hay PJ. Ab initio effective core potentials for molecular calculations. Potentials for main group elements Na to Bi. J Chem Phys 1985;82(1):284–98.
[24] Chen N, Yang RT. Ab initio molecular orbital study of the unified mechanism and pathways for gas–carbon reactions. J Phys Chem A 1998;102(31):6348–56.
[25] Chen N, Yang RT. Ab initio molecular orbital calculation on graphite: selection of molecular system and model chemistry. Carbon 1998;36(7–8):1061–70.
[26] Butkus AM, Fink WH. Ab initio model calculations for graphite: bulk and basal plane electronic densities. J Chem Phys 1980;73(6):2884–92.
[27] Hu Q, Wu Q, Sun G, Luo X, Liu Z, Xu B, et al. First-principles study of atomic oxygen adsorption on boron-substituted graphite. Surf Sci 2008;602:37–45.

[28] Menendez JA, Xia B, Phillips J, Radovic LR. On the modification and characterization of chemical surface properties of activated carbon: microcalorimetric, electrochemical, and thermal desorption probes. Langmuir 1997;13:3414–21.
[29] Olson ES, Laumb JD, Benson SA, Dunham GE, Sharma RK, Mibeck BA, Miller SJ, et al. An improved model for flue gas–mercury interactions on activated carbons. In: Proceedings of mega symposium and air and waste management association's specialty conference. Washington, DC; 2003.
[30] Weast RC, editor. Handbook of chemistry and physics. 61st ed. Cleveland OH: CRC Press; 1978.
[31] Perez-Cadenas AF, Maldonado-Hodar FJ, Moreno-Castilla C. On the nature of surface acid sites of chlorinated activated carbons. Carbon 2003;41(3):473–8.
[32] Nilsson A, Pettersson LGM. Adsorbate electronic structure and bonding on metal surfaces. In: Nilsson A, Pettersson LGM, Norskov JK, editors. Chemical bonding at surfaces and interfaces. Amsterdam, The Netherlands: Elsevier; 2008. p. 57–138.